ORIGINAL ARTICLE
Cell Therapy & Organ Transplantation

JKMS

http://dx.doi.org/10.3346/jkms.2015.30.9.1232 • J Korean Med Sci 2015; 30: 1232-1240

Preserved Hippocampal Glucose Metabolism on ^{18}F-FDG PET after Transplantation of Human Umbilical Cord Blood-derived Mesenchymal Stem Cells in Chronic Epileptic Rats

Ga Young Park,[1,7] Eun Mi Lee,[2] Min-Soo Seo,[3] Yoo-Jin Seo,[3] Jungsu S. Oh,[4] Woo-Chan Son,[5] Ki Soo Kim,[6] Jae Seung Kim,[4] Joong Koo Kang,[1] and Kyung-Sun Kang[3]

[1]Department of Neurology, University of Ulsan College of Medicine, Asan Medical Center, Seoul; [2]Department of Neurology, Ulsan University Hospital, Ulsan; [3]Adult Stem Cell Research, College of Veterinary Medicine, Seoul National University, Seoul; [4]Department of Nuclear Medicine, [5]Department of Pathology, and [6]Department of Pediatrics, University of Ulsan College of Medicine, Asan Medical Center, Seoul; [7]The Asan Institute for Life Science, Seoul, Korea

Received: 15 September 2014
Accepted: 18 May 2015

Address for Correspondence:
Joong Koo Kang, MD
Department of Neurology, University of Ulsan College of Medicine, Asan Medical Center, 88 Olympic-ro 43-gil, Songpa-gu, Seoul 138-736, Korea
Tel: +82.2-3010-3448, Fax: +82.2-474-4691
E-mail: jkkang@amc.seoul.kr

Funding: This research was fully supported by the Asan Institute for Life Science, Seoul, Korea (contract 09-338) and the Bio & Medical Technology Development Program of the National Research Foundation (No. 2010-0020265), which is funded by the Korean Government.

Human umbilical cord blood-derived mesenchymal stem cells (hUCB-MSCs) may be a promising modality for treating medial temporal lobe epilepsy. ^{18}F-fluorodeoxyglucose positron emission tomography (FDG-PET) is a noninvasive method for monitoring in vivo glucose metabolism. We evaluated the efficacy of hUCB-MSCs transplantation in chronic epileptic rats using FDG-PET. Rats with recurrent seizures were randomly assigned into three groups: the stem cell treatment (SCT) group received hUCB-MSCs transplantation into the right hippocampus, the sham control (ShC) group received same procedure with saline, and the positive control (PC) group consisted of treatment-negative epileptic rats. Normal rats received hUCB-MSCs transplantation acted as the negative control (NC). FDG-PET was performed at pre-treatment baseline and 1- and 8-week posttreatment. Hippocampal volume was evaluated and histological examination was done. In the SCT group, bilateral hippocampi at 8-week after transplantation showed significantly higher glucose metabolism (0.990 ± 0.032) than the ShC (0.873 ± 0.087; $P < 0.001$) and PC groups (0.858 ± 0.093; $P < 0.001$). Histological examination resulted that the transplanted hUCB-MSCs survived in the ipsilateral hippocampus and migrated to the contralateral hippocampus but did not differentiate. In spite of successful engraftment, seizure frequency among the groups was not significantly different. Transplanted hUCB-MSCs can engraft and migrate, thereby partially restoring bilateral hippocampal glucose metabolism. The results suggest encouraging effect of hUCB-MSCs on restoring epileptic networks.

Keywords: Lithium-pilocarpine; Positron-emission Tomography; Animal Model of Chronic Epilepsy; Mesenchymal Stem Cell Transplantation; Cell Therapy

INTRODUCTION

Epilepsy is a chronic disorder characterized by spontaneous recurrent seizures (SRS). Currently, there is no effective treatment that prevents or restrains the development or progression of this condition. Medial temporal lobe epilepsy (MTLE) is a possible clinical target for stem cell-based therapies that suppress or restrain the progression of chronic epilepsy (1). Self-renewing neural stem cells can differentiate into neurons and glial cells, which can repair damaged neuronal tissue and form functional neuronal circuitry. A recent study reported that human fetal-derived neural stem cells that are transplanted into injured hippocampus can differentiate into gamma-aminobutyric acid (GABA)-synthesizing cells, thereby reducing seizure frequency in a pilocarpine model of MTLE (2). Human umbilical cord blood-derived mesenchymal stem cells (hUCB-MSCs) demonstrate many advantages over embryonic and adult stem cells: they are less ethically controversial (with few legal constraints) and easy to collect using noninvasive procedures. Many studies suggest that hUCB-MSCs can differentiate into neural cells and may demonstrate neurotrophic effects and therapeutic potential against neurological disease (3).

hUCB-MSCs transplantation may be used to treat medically resistant MTLE that cannot be surgically treated. The ability to restore function is highly desirable from a clinical standpoint, but chronically damaged areas of the brain may be a particularly hostile environment for engrafted cells. It remains unknown if stem cell transplantation benefits chronic epilepsy models with established epileptogenic circuitry. Thus, assessment of the practical applications and therapeutic potential of stem cell transplantation in an established model of chronic epilepsy (as opposed to the acute period after status epilepticus [SE]) are needed.

Evaluating longitudinal functional and molecular changes

pISSN 1011-8934
eISSN 1598-6357

can help understand serial changes in disease pathogenesis and assess treatment efficacy in neurologic conditions, including epilepsy (4-8). Unlike postmortem analyses, where observations are limited to specific time points following insult, ^{18}F-fluorodeoxyglucose positron emission tomography (FDG PET) can be used to monitor in vivo glucose metabolism and assess brain processing over time, including those related to epileptogenesis (8). Assessing hippocampal glucose metabolism before and after treatment may help predict the therapeutic efficacy of hUCB-MSCs transplantation (9).

The aim of this study was to evaluate hippocampal glucose metabolism after hUCB-MSCs transplantation using serial FDG PET monitoring in a lithium-pilocarpine model of chronic epilepsy. We also assessed any correlations of hUCB-MSCs transplantation with histopathology and clinical improvement.

MATERIALS AND METHODS

Epilepsy model and experimental design

Experimental design is illustrated in Fig. 1. Male Sprague Dawley rats (10 weeks old; approximately 300 g) were housed under standard laboratory conditions (22-24°C; 12-hr light/dark cycle). Lithium-pilocarpine was used to induce SE, as previously described (8). Ten weeks after the induction of SE, rats with SRS were randomly assigned to three groups: the stem cell treatment (SCT) group received hUCB-MSCs transplantation (n = 8); the sham control (ShC) group received sham surgery and the same amount of phosphate-buffered saline (PBS) instead of hUCB-MSCs transplantation (n = 9); and the positive control (PC) group consisted of treatment-naïve post-SE rats (n = 9). In addition, 20-week-old normal rats did not undergo SE but did receive hUCB-MSCs transplantation and acted as the negative control (NC) group (n = 7).

The SCT and NC groups received hUCB-MSCs transplantation using a stereotaxic apparatus and syringe pump (Nanomite; Harvard Apparatus, Miami, FL, USA). hUCB-MSCs suspensions (5×10^5/2 μL) were injected over a period of 5 min using a 5-μL Hamilton syringe (Hamilton company, Reno, NV, USA) that was placed in the right hippocampus (coordinates: AP -4.3 mm; L -3.5 mm; depth -4.0 mm). The same procedure was performed on the ShC group using an equal amount of PBS. The infused volume was 2 μL, and the rate of infusion was 0.5 μL/min. The PC group received neither stem cell transplantation nor surgery. Aseptic techniques were strictly followed during all animal experiments. The rats were maintained under postoperative care for 1 week and did not receive any immunosuppressant.

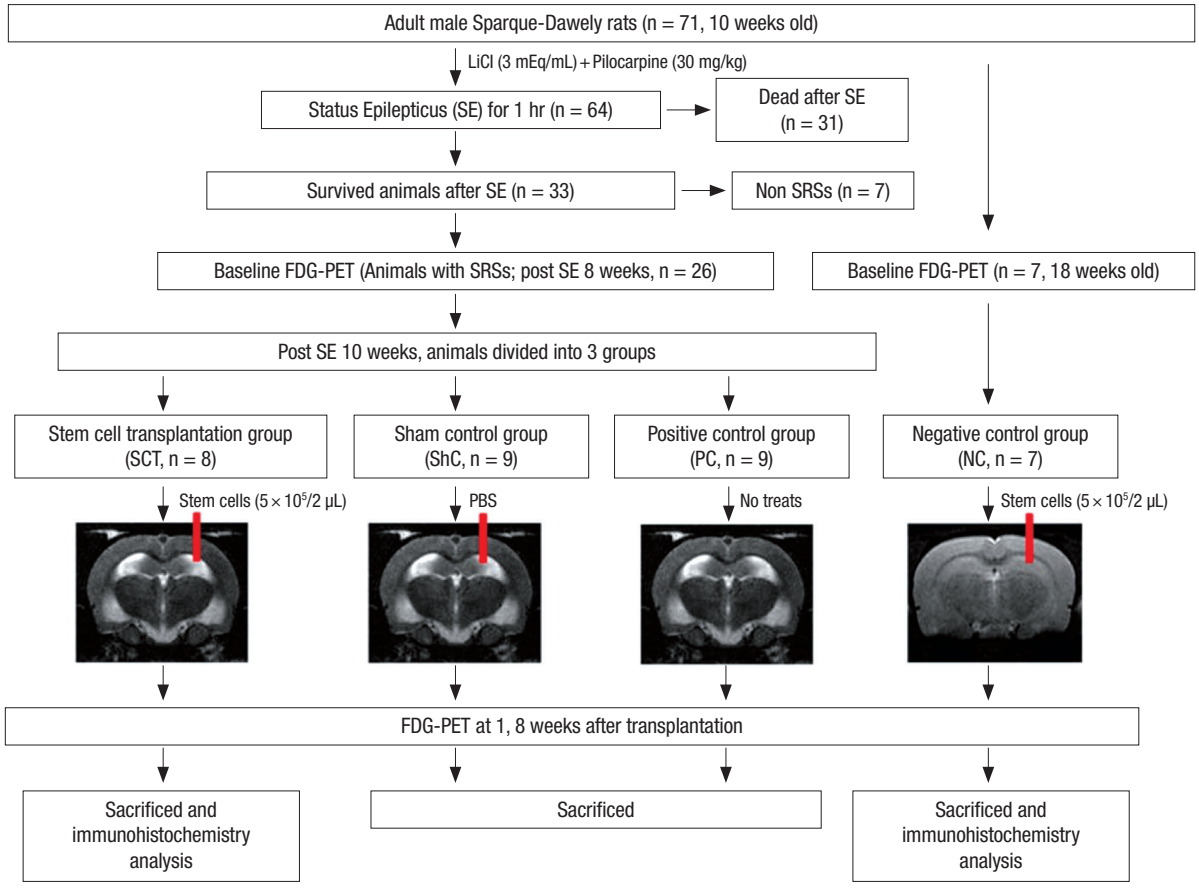

Fig. 1. Schematic depicting the evaluation of changes in hippocampal glucose metabolism using ^{18}F-FDG PET after hUCB-MSCs transplantation in chronic epileptic rats.

Extract preparation and hUCB-MSCs transplantation

hUCB samples were obtained from the Seoul City Borame Hospital Cord Blood Bank (Seoul, Korea) and cultured, as previously described (10), with the approval of the Borame Hospital Institutional Board and Seoul National University (Seoul, Korea) (IRB No. 0603/001-002-07C1). To track the injected hUCB-MSCs, the cells were labeled with PKH-26, a lipophilic marker that is taken up by viable cell membranes (11). This marker allowed us to identify transplanted cells in the SCT and NC groups after sacrifice.

PET imaging

Food was withdrawn 20 hr before scanning so the PET data would be acquired under controlled metabolic conditions. Rats were anesthetized with 1.5%-2% isoflurane in air (2 L/min) for 20 min before administering an intravenous injection of ^{18}F-FDG (37 MBq/rat) into the tail vein; 1.5%-2% isoflurane was maintained until the end of PET acquisition. PET scans were performed as described in our previous paper (8). We did not conduct PET on the scheduled imaging day if the rats exhibited definite clinical seizures. In this situation, animals were imaged at least 2-3 days later.

All animals were scanned using FDG PET at three time points (Fig. 1): 1) 8-week post-SE for the SCT, ShC, and PC groups, or 18 weeks for the NC group, for use as baseline; 2) 1-week posttransplantation in the SCT, NC, and ShC groups, or 11 weeks post-SE for the PC group; and 3) 8-week posttransplantation in the SCT, NC, and ShC groups, or 18 weeks post-SE for the PC group.

Region of interest analysis

Regions of interest (ROIs) were defined on the reconstructed images in order to estimate regional ^{18}F-FDG uptake. We manually defined ROIs in two specific regions (bilateral hippocampus and pons; Fig. 2) using a rat brain atlas-based MRI template (12) and MRIcro (Neuropsycology Lab, Columbia, SC, USA). Defining ROIs was done as explained in our previous work (8). Three investigators collaborated to define ROIs accurately; all included ROIs were determined by consensus. We laid the ROI template onto each normalized PET image and reconfirmed visually that the PET image corresponded to the anatomical locations on the template. This was performed in a manner so that the investigators were blind to all groups, including the treatment groups. We only evaluated ROIs in the bilateral hippocampi, which is the most important epileptic zone in MTLE. We also performed a subanalysis of the ROI results to ensure comparability between unilateral and bilateral ROI data.

FDG PET images were normalized to the administered radioactive dose. We calculated the concentration of a radioactive tracer in a given region with the percent injected dose per milliliter (%ID/mL). It is a useful semiquantitative measurement using the following equation: %ID/mL = mean tissue concentration (MBq/mL)/injected dose (MBq) × 100%. The metabolic rate of glucose in the hippocampus was normalized to the pons glucose and is reported as the mean ± standard error of the mean (SEM). Because the metabolic rate of pons is unaffected by lithium-pilocarpine induced seizures, it was chosen for normalization (8, 13-16). We analyzed the metabolic rate in the pons in each the four groups and confirmed no significant differences (data not shown). Due to individual variability in baseline glucose metabolism, changes between the three time points are expressed as the relative percent change compared with hippocampal baseline (100%): ($\text{changes}_{\text{x-baseline}}$ = [glucose metabolic rate_{x}-glucose metabolic $\text{rate}_{\text{baseline}}$]/glucose metabolic $\text{rate}_{\text{baseline}}$ × 100) (x = 1- or 8-week posttreatment).

MRI acquisition

MRI acquisition was performed as described in our previous study (8). The MRI and PET studies were performed on the SCT, ShC, and PC groups at the same time.

Hippocampal volume analysis

We performed hippocampal volume analyses of the SCT, ShC, and PC groups at different time points in order to exclude partial volume effects. Volume analysis was performed using ImageJ software (freeware version 1.44, developed by Wayne Rasband, NIH; http://rsb.info.nih.gov/ij). Volumetric analysis was performed on three coronal slices at the level of the cingulate cortex, dorsal hippocampus, and ventral hippocampus (Fig. 2). Volume was estimated using the following formula: hippocampal volume = sum of the hippocampal area of each slice × 1.5 mm (slice thickness). Hippocampal volume (μL) is expressed as the mean ± SEM.

SRS monitoring

Between 4-week post-SE and 8-week posttransplantation (or

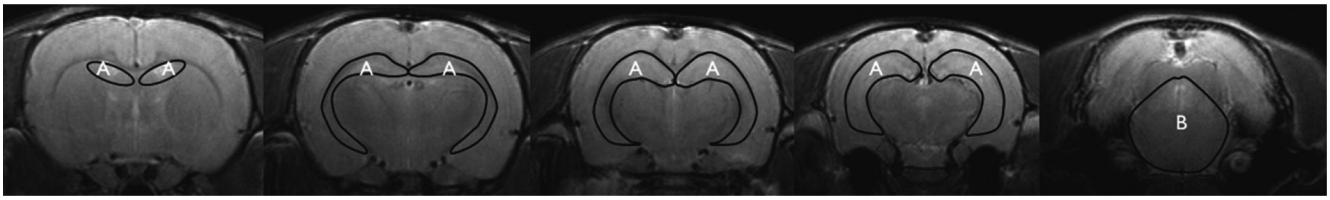

Fig. 2. Representative regions of interest (ROIs) drawn on coronal T2-weighted MRI. (**A**) Hippocampus. (**B**) Pons.

 http://dx.doi.org/10.3346/jkms.2015.30.9.1232

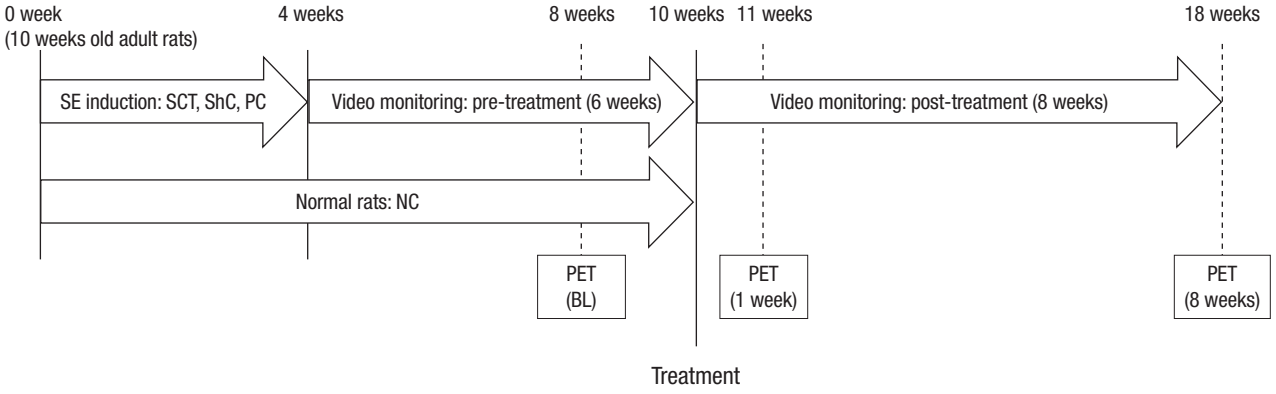

Fig. 3. Schematic illustration of the monitoring period.

18-week post-SE), the surviving rats were monitored with a video recorder (6 hr/day, 3 days/week) to assess SRS. An illustration of the monitoring period is shown in Fig. 3. Only rats in the SCT, ShC, and PC groups with ≥ 2 SRS after the latent period or before transplantation were included in this experiment. Since we only evaluate the SRS with video recording, only stage 4 or 5 convulsive seizures according to the Racine's scale were evaluated in our study. We evaluated the frequency of SRS. We compared seizure status in the pretreatment (4-10-week post-SE) and posttreatment periods (0-8-week posttreatment) in the SCT, ShC, and PC groups.

Histopathology

After performing FDG PET at 8-week posttransplantation, the SCT and NC animals were anesthetized with a mixture of ketamine-xylazine and the left heart ventricle was perfused with 4% freshly prepared paraformaldehyde. Rats in the PC groups were also sacrificed at 18-week post-SE using the same method. Brains were removed and postfixed for a day in the same fixative at 4°C, and the tissues were separated for immunohistochemical processing. Brains were cryoprotected in 30% sucrose for another 48 hr in order to assess neuronal differentiation (n = 3; SCT and NC groups). Immunohistochemistry was performed using primary antibodies for antimicrotubule-associated protein 2 (MAP2) and antiglial fibrillary acidic protein (GFAP) (Millipore, Billerica, MA, USA) (10). The sections were extensively washed with PBS and incubated for 1 hr with anti-mouse or anti-rabbit secondary antibodies that were conjugated with Alexa Fluor 488 or 594 (Molecular Probes, Eugene, OR, USA), followed by Hoechst 33238 (1 μg/mL; Sigma-Aldrich, St. Louis, MO, USA) or DAPI staining (10 μg/mL; Invitrogen, Carlsbad, CA, USA) in order to visualize cell nuclei. A confocal microscope (Eclipse TE200; Nikon, Tokyo, Japan) was used to capture all images.

To evaluate inflammatory changes in the hippocampus, tissues were embedded with paraffin, cut into 3-μm-thick sections, and mounted on glass slides (n = 4; SCT and PC groups). An automated slide preparation system (Benchmark XT; Ventana Medical systems Inc, Tucson, AZ, USA) was used for immunohistochemistry. Deparaffinization, epitope retrieval, and immunostaining were performed using cell conditioning solution (CC1) and the BMK ultraVIEW diaminobenzidine (DAB) detection system (Ventana Medical Systems) according to the manufacturer's instructions. Microglial cells were stained with rabbit anti-Iba1 (1:200; Wako, Osaka, Japan) and ultra-VIEW copper amplified the positive signals. Sections were counterstained with bluing reagent and hematoxylin. To estimate the number of Iba1-expressing microglial cells, images of the ventral hippocampus were captured using an Olympus BX53 microscope and cell sens standard program (Tokyo, Japan). Iba1-expressing microglial cells were counted in two areas in each of the three ROIs within the hippocampus including dendrite gyrus (DG), CA1, and CA3 (400 × magnification). Entirely contained cells within each section were counted to avoid double counting within consecutive sections. Two blind observers quantified the microglial cells.

Statistical analysis

Numerical data are presented as the mean ± SEM. The paired *t*-test, repeated-measures ANOVA, Kruskal-Wallis test, and Wilcoxon signed-rank tests were performed using SPSS (version 18.0; SPSS, Inc., Chicago, IL, USA). The level of statistical significance was set at $P < 0.05$. A linear mixed-effect model (SAS 9.1; SAS Institute Inc., Cary, NC, USA) was used to accommodate within- and between-subject sources of variation.

Ethics statement

All experimental procedures were performed in accordance with the National Institutes of Health (NIH) Guidelines for the care and use of laboratory animals. The study protocol was approved by institute animal care and use committee of Asan Medical Center Research Authority, Seoul, Korea (IACUC; 2009-03-015).

RESULTS

Glucose metabolism

Hippocampal glucose metabolism was normalized to the pons. Comparisons of glucose metabolism are provided in Table 1 and Fig. 4. Hippocampal glucose metabolism was significantly different at 8-week posttreatment between the four groups. Glucose metabolism at 8-week posttreatment was significantly higher in the SCT group (0.990 ± 0.032) than the ShC (0.873 ± 0.087; $P < 0.001$) and PC groups (0.858 ± 0.093; $P < 0.001$), but hippocampal glucose metabolism in the SCT group was not restored to NC baseline (1.109 ± 0.021), even by 8-week posttreatment (1.094 ± 0.013). The SCT group demonstrated a gradual increase in glucose metabolism compared with baseline, but this finding was not statistically significant. However, the ShC and PC groups demonstrated markedly decreased glucose metabolism at 8-week posttreatment ($P = 0.04$ and 0.01, respectively). Glucose metabolism in the NC group decreased by 1-week posttransplantation, but recovered to baseline by 8-week posttreatment. However, the NC group did not demonstrate increased glucose metabolism at 8-week posttreatment compared with baseline, in contrast to the SCT group (Fig. 4 and Table 1). In addition, unilateral changes in glucose metabolism in the hippocampus were similar to the bilateral results at each time point, and there was no significant difference between the ipsilateral (injected side) and contralateral sides (data not shown).

Hippocampal volume

Hippocampal volume was assessed at each time point (Table 2). There were no significant differences between the groups at any time point.

Survival and distribution of grafted MSC

Rats in the SCT and NC groups were assessed using histological examination. The location and appearance of the PKH26-labeled cells were evaluated to determine the viability and differentiation potential of transplanted hUCB-MSCs. PKH26-labeled hUCB-MSCs were observed in the ipsilateral and contralateral hippocampus in the SCT and NC groups, but they did not differentiate into neuronal cells or glial cells in either group (Fig. 5).

Quantification of microglial activation

To evaluate inflammatory effects, Iba1-labeled microglial cells in the SCT and PC groups were counted in bilateral hippocampi (Fig. 6). In total, 204.3 ± 36.95 and 221 ± 40.8 Iba1-labeled microglial cells were counted in the bilateral hippocampi of the SCT and PC groups, respectively, but this difference is not statistically significant. The number of Iba1-labeled microglial cells was not statistically different between the left and right sides in each group.

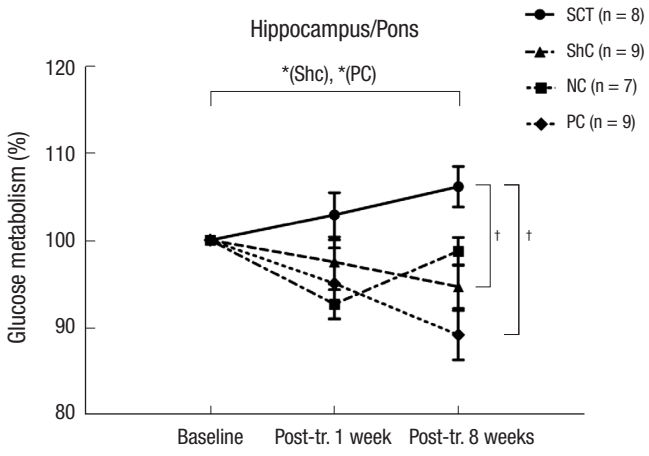

Fig. 4. Glucose metabolism in the experimental and control groups. Hippocampal glucose metabolism at each of the three time points is expressed as the relative percent change compared with baseline (100%). *$P < 0.05$; †$P < 0.01$.

Table 1. Glucose metabolism in rat hippocampus normalized to the pons

	SCT	ShC	NC	PC
Baseline	0.936 ± 0.037	0.926 ± 0.131*	1.109 ± 0.021	0.966 ± 0.098*
1-week posttreatment	0.960 ± 0.032	0.903 ± 0.089	1.028 ± 0.021	0.921 ± 0.097
8-week posttreatment	0.990 ± 0.032$^{ShC, PC}$	0.873 ± 0.087$^{SCT, *}$	1.094 ± 0.013^{PC}	0.858 ± 0.093$^{SCT, NC, *}$

All values indicate the mean ± SEM. Results are expressed as %ID/mL ratio. All statistical analyses were performed using linear mixed-effects modeling. *Significantly different from the other time points in the same group ($P < 0.05$). $^{SCT, ShC, NC, PC}$Difference ($P < 0.01$) in comparison with the designated group at the same time point (SCT, stem cell treatment group; ShC, sham control group; NC, normal control group; PC, positive control group).

Table 2. Bilateral hippocampal volume (μL)

	SCT		ShC		PC	
	Left	Right	Left	Right	Left	Right
Baseline	30.32 ± 1.62	31.03 ± 1.16	30.92 ± 1.11	31.13 ± 0.84	29.42 ± 1.1	29.4 ± 0.98
1-week posttreatment	30.02 ± 1.4	28.68 ± 1.07	31.22 ± 1.22	29.97 ± 0.92	28.97 ± 1.18	27.86 ± 1.37
8-week posttreatment	29.11 ± 1.2	29.54 ± 1.23	30.39 ± 1.19	28.87 ± 1.03	27.62 ± 1.37	27.52 ± 1.28

All results indicate the mean ± SEM. Bilateral hippocampal volume demonstrated no significant differences within or between groups. SCT, stem cell treatment group; ShC, sham control group; PC, positive control group.

http://dx.doi.org/10.3346/jkms.2015.30.9.1232

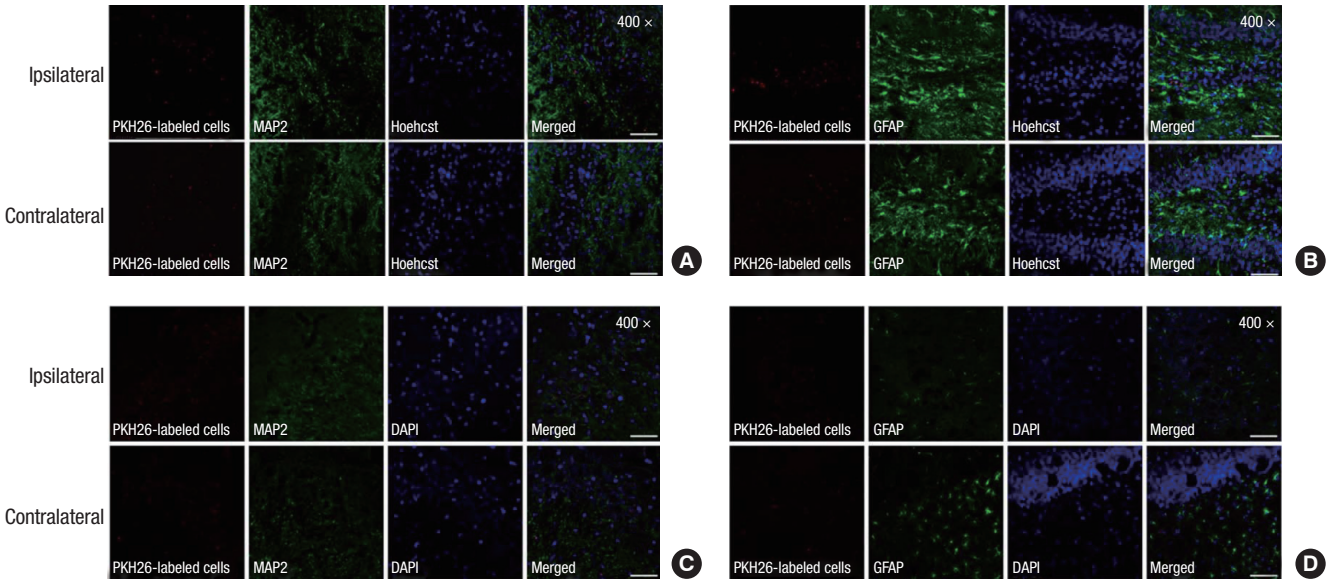

Fig. 5. Transplanted hUCB-MSCs in the bilateral hippocampus of the SCT and NC groups. (**A**, **B**) Immunohistochemical analysis of the SCT group. (**C**, **D**) Immunohistochemical analysis of the NC group. Red indicates transplanted hUCB-MSCs labeled with PKH26 (PKH26-labeled cells). (**A**, **C**) Neurons labeled with anti-MAP2. (**B**, **D**) Astrocytes labeled with anti-GFAP (upper panel, ipsilateral; lower panel, contralateral). Scale bar, 100 μm.

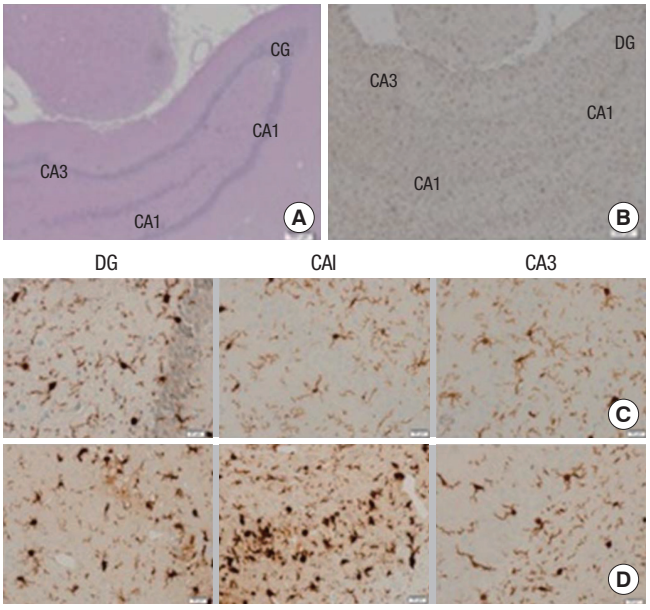

Fig. 6. Iba1-labeled microglial cells. Right ventral hippocampal cut of (**A**) hematoxylin-eosin and (**B**) Iba1 stains in SCT group to confirm the ROIs (40 × magnification). Iba1-expressing microglial cells were counted at 400 × magnification in the bilateral hippocampi. Microglial cells in right hippocampus are shown in (**C**) the SCT group and (**D**) PC group. Scale bar, 200 μm (**A**, **B**) or 20 μm (**C**, **D**).

Behavioral changes and seizure frequency

Sixty-four rats were treated with pilocarpine and developed SE. Of these, 33 survived (51.6%) to 10-week post-SE and SRS developed in 26 of 33 animals (78.8%) within 41 ± 6.3 days (range: 36-49 days). We monitored 26 rats using a video recorder for 14 weeks (4-18-week post-SE or 8-week posttreatment). Seizure frequencies demonstrated no significant differences between pre- and post-treatment across all three groups (P = 0.88; Table 3). In addition, our subanalysis of the SCT, ShC, and PC group demonstrated no significant difference between pre- and post-treatment (P = 0.67, 0.44, and 0.59, respectively).

Table 3. Seizure frequency (seizures/day)

Group	Seizure/day	
	Pretreatment	Posttreatment
SCT	0.80 ± 0.18	0.82 ± 0.15
ShC	0.74 ± 0.19	0.85 ± 0.19
PC	0.86 ± 0.16	0.91 ± 0.17

All results indicate the mean ± SEM. Seizure frequency analysis indicates no significant changes between pre- and posttreatment. SCT, stem cell treatment group; ShC, sham control group; PC, positive control group.

DISCUSSION

We here evaluate the therapeutic potential of hUCB-MSCs transplantation in a lithium-pilocarpine rat model of chronic epilepsy and assess in vivo functional efficacy using longitudinal PET imaging. To our knowledge, this is the first study to compare longitudinal metabolic changes following hUCBs-MSCs transplantation in a clinically relevant model of chronic epilepsy. Bilateral hippocampal glucose metabolism increased in the SCT group by 8-week posttransplantation compared with baseline, but this level never recovered to the baseline of the NC group; hippocampal glucose metabolism at 8-week posttreatment decreased in the ShC and PC groups compared with baseline. Histological examination revealed that the transplanted hUCB-MSCs in the SCT group survived in the ipsilateral and contra-

lateral hippocampi but did not differentiate. These findings suggest that transplanted hUCB-MSCs can migrate to the damaged hippocampus and partially restore bilateral hippocampal glucose metabolism, but the engrafted hUCB-MSCs did not restore epileptogenic circuitry or alter the clinical course.

Our current study data show that hUCB-MSCs demonstrate powerful migratory activities, moving from the primary implantation site to the contralateral hippocampus in both the chronic epilepsy model and normal rats, despite the fact that the chronic epilepsy model is supposedly a hostile environment for stem cell survival and proliferation. The therapeutic efficacy of transplantation has been reported in the acute period within days or weeks after SE (17). Acute injury may transiently stimulate the release of tropic factors and chemokines that promote survival, migration, and the integration of transplanted stem cells. In contrast, the low survival rate of these transplanted cells in chronic epilepsy models has generally been attributed to the low concentration of trophic factors and decreased vascularity of damaged tissue. Here, we performed hUCB-MSCs transplantation on chronic epileptic rats at 10-week post-SE, demonstrating that hUCB-MSCs engraftment is feasible.

Hippocampal glucose metabolism in the SCT group remained stable for at least 8-week posttransplantation in comparison with baseline, whereas hippocampal glucose in the ShC and PC groups gradually decreased or remained unchanged in the NC group compared with baseline. These findings suggest that stem cell transplantation plays a critical role in preventing progressive hypometabolism. Although we did not demonstrate complete functional recovery or clinical improvement, preserved glucose uptake in bilateral hippocampi indicates long-term stem cell survival, possibly due to neurotrophic factors that are secreted from these cells and mitigate the effects of progressive hypometabolism. This effect was not due to changes in hippocampal volume, which was not significantly different at any time point. Therefore, differences in hippocampal metabolism cannot be explained by differences in hippocampal volume between groups.

It could be argued that increased glucose metabolism in the SCT group resulted from the inflammatory effects of the hUCB-MSCs or surgical manipulation. It is well known that FDG PET can demonstrate false-positive uptake in the presence of inflammation. A previous study reported that high glucose metabolism at 7-day postischemia on FDG PET is caused by inflammation, including microglial cell activation. However, glucose metabolism decreased in the ShC group, whereas glucose metabolism was maintained or slightly increased at 8-week posttreatment in the SCT group, which suggests that this result cannot be attributed to surgical manipulation. In addition, increased glucose metabolism at 8-week posttransplantation was greater than at 1-week posttransplantation in the SCT group, which cannot be explained by the acute inflammatory effects of SCT or surgical manipulation. Furthermore, immunohistochemical staining in the present study indicates no difference in the number of microglial cells in the hippocampus between the SCT and PC groups. Therefore, the inflammatory effects of surgery and hUCB-MSCs cannot explain increased glucose metabolism compared with baseline in the SCT group.

The most probable explanation of increased glucose metabolism compared with baseline in the SCT group is the positive metabolic effects of hUCB-MSCs. In the PC group, the decrease in glucose metabolism observed at 18-week post-SE (equivalent to 8-week posttreatment) may have been due to the progression of epileptogenesis, even though there were no statistically significant differences in seizure frequency compared with baseline. This is supported by the fact that the decrease in hippocampal glucose metabolism progressively expanded to the entire limbic area during the chronic period (8-week post-SE), which suggests that glucose metabolism decreases in chronic epileptogenesis (8). Hypometabolism may be associated with tissue degeneration and cell loss in those areas, or it may occur independent of hippocampal volume loss (18-20). However, it is well known that hippocampal hypometabolism in epilepsy is correlated with epileptic networks, including epileptic foci (21-24), and decreases in hypometabolic areas have been observed in patients with decreased seizure frequency (25, 26). In the present study, we only evaluated hippocampal glucose metabolism because the hippocampus is the area of the brain that most commonly generates epileptic seizures in MTLE. Thus, in the present study, the maintenance of glucose metabolism in the SCT group in contrast to progressive hypometabolism in ShC and PC groups imply that hUCB-MSCs may affect epileptic networks, even though differences in the seizure frequency were not statistically significant.

Therapeutic stem cell transplantation replaces damaged cells and provides a better microenvironment for endogenous cells by providing paracrine effects (10). Therefore, it is possible to protect against inflammatory damage in order to repair or rebuild host networks and circuits (27, 28). In our current analyses, hUCB-MSCs migrated to the contralateral hippocampus where they remained undifferentiated. Although transplanted hUCB-MSCs did not differentiate into specific neuronal cell types, they did affect the maintenance of glucose metabolism. However, we could not identify the factors produced by hUCB-MSCs that allow maintenance or increase glucose metabolism, or determine if novel synaptic formation or neuronal circuitry were integrated into the adjacent brain tissue. Further studies are needed to answer these questions.

Some researchers argue that isoflurane affects the cerebral uptake of FDG. However, several studies on PET imaging have been performed using isoflurane anesthesia (8, 20, 29). Here, we compared the results of PET scanning between the 4 groups, which were taken using the same conditions of isoflurane an-

 http://dx.doi.org/10.3346/jkms.2015.30.9.1232

esthesia, and used the pons as the standard for normalization in each rat because the metabolic rate of the pons is unaffected by pilocarpine-induced seizures (13-16). Thus, we believe our comparisons are reasonable, even though isoflurane anesthesia may have hampered FDG uptake.

This study has several limitations. First, the intravenous induction of SE results in widespread brain damage, which creates a poor microenvironment for hUCB-MSCs. In future studies, it may be more efficient to use a focal epilepsy model to assess improvements following hUCB-MSCs transplantation. Second, we did not perform electroencephalography (EEG) monitoring with implanted electrodes to evaluate seizure frequency because implanted electrodes make it impossible to perform MRI and may affect PET metabolism. Seizure frequency and severity were evaluated by video recording thus the mild electrographic or clinical seizures could be overlooked in the present study. Third, although we performed follow-up examinations at 8-week posttransplantation, we still need to assess the long-term effects of hUCB-MSCs transplantation. Finally, we could not identify the exact reason or factors that preserved or increased glucose metabolism after stem cell transplantation. The secretion of neurotrophic factors by hUCB-MSCs was not confirmed in this in vivo study. We think that revealing these issues are another important subject for further study.

In conclusion, this study demonstrated that hUCB-MSCs that were injected into the hippocampus of rats with chronic epilepsy would engraft, survive, and appeared to maintain hippocampal glucose metabolism. These results suggest the possible promising effects of hUCB-MSCs on epileptic networks, even though they did not restore epileptogenic circuitry or alter the clinical course in the present experiments.

ACKNOWLEDGEMENTS

We thank Sang Tae Kim and Chul-Woong Woo who are researchers at The Asan Institute for Life Science for their assistance with MRI acquisition and Jin Hwa Chung and Yeseulmi Kim, also researchers at The Asan Institute for Life Science for their assistance with PET acquisition.

DISCLOSURE

The authors have no conflicts of interest to disclose.

AUTHOR CONTRIBUTION

Designed the study: Kang JK, Kang KS. Performed the study: Park GY, Seo YJ, Seo MS, Lee EM. Data preparation: Oh JS, Park GY, Seo YJ, Seo MS. Data analysis: Park GY, Son WC, Kim KS, Kim JS. Lee EM, Kang JK, Kang KS. Data visualization: Park GY. Manuscript preparation: Park GY, Lee EM, Kang JK, Kang KS. Manuscript approval: all authors. Supervision of the study: Kang JK.

ORCID

Ga Young Park *http://orcid.org/0000-0002-0560-9638*
Eun Mi Lee *http://orcid.org/0000-0001-6423-0081*
Min-Soo Seo *http://orcid.org/0000-0002-2840-9831*
Yoo-Jin Seo *http://orcid.org/0000-0001-8159-7918*
Jungsu S. Oh *http://orcid.org/0000-0002-1925-8103*
Woo-Chan Son *http://orcid.org/0000-0002-4052-8745*
Ki Soo Kim *http://orcid.org/0000-0003-1547-5220*
Jae Seung Kim *http://orcid.org/0000-0003-1710-1185*
Joong Koo Kang *http://orcid.org/0000-0003-0941-3824*
Kyung-Sun Kang *http://orcid.org/0000-0002-9322-741X*

REFERENCES

1. Hattiangady B, Rao MS, Shetty AK. *Grafting of striatal precursor cells into hippocampus shortly after status epilepticus restrains chronic temporal lobe epilepsy. Exp Neurol 2008; 212: 468-81.*
2. Chu K, Kim M, Jung KH, Jeon D, Lee ST, Kim J, Jeong SW, Kim SU, Lee SK, Shin HS, et al. *Human neural stem cell transplantation reduces spontaneous recurrent seizures following pilocarpine-induced status epilepticus in adult rats. Brain Res 2004; 1023: 213-21.*
3. Yang CC, Shih YH, Ko MH, Hsu SY, Cheng H, Fu YS. *Transplantation of human umbilical mesenchymal stem cells from Wharton's jelly after complete transection of the rat spinal cord. PLoS One 2008; 3: e3336.*
4. van Eijsden P, Notenboom RG, Wu O, de Graan PN, van Nieuwenhuizen O, Nicolay K, Braun KP. *In vivo 1H magnetic resonance spectroscopy, T2-weighted and diffusion-weighted MRI during lithium-pilocarpine-induced status epilepticus in the rat. Brain Res 2004; 1030: 11-8.*
5. Niessen HG, Angenstein F, Vielhaber S, Frisch C, Kudin A, Elger CE, Heinze HJ, Scheich H, Kunz WS. *Volumetric magnetic resonance imaging of functionally relevant structural alterations in chronic epilepsy after pilocarpine-induced status epilepticus in rats. Epilepsia 2005; 46: 1021-6.*
6. Kuo LW, Lee CY, Chen JH, Wedeen VJ, Chen CC, Liou HH, Tseng WY. *Mossy fiber sprouting in pilocarpine-induced status epilepticus rat hippocampus: a correlative study of diffusion spectrum imaging and histology. Neuroimage 2008; 41: 789-800.*
7. Yakushev IY, Dupont E, Buchholz HG, Tillmanns J, Debus F, Cumming P, Heimann A, Fellgiebel A, Luhmann HJ, Landvogt C, et al. *In vivo imaging of dopamine receptors in a model of temporal lobe epilepsy. Epilepsia 2010; 51: 415-22.*
8. Lee EM, Park GY, Im KC, Kim ST, Woo CW, Chung JH, Kim KS, Kim JS, Shon YM, Kim YI, et al. *Changes in glucose metabolism and metabolites during the epileptogenic process in the lithium-pilocarpine model of epilepsy. Epilepsia 2012; 53: 860-9.*
9. Zhai Q, Gui J, Zhang Y, Qiao H. *Children treated for epileptic encephalopathies show improved glucose metabolism. Pediatr Int 2010; 52: 883-7.*
10. Seo Y, Yang SR, Jee MK, Joo EK, Roh KH, Seo MS, Han TH, Lee SY, Ryu PD, Jung JW, et al. *Human umbilical cord blood-derived mesenchymal stem cells protect against neuronal cell death and ameliorate motor deficits in Niemann Pick type C1 mice. Cell Transplant 2011; 20: 1033-47.*

11. Wisenberg G, Lekx K, Zabel P, Kong H, Mann R, Zeman PR, Datta S, Culshaw CN, Merrifield P, Bureau Y, et al. *Cell tracking and therapy evaluation of bone marrow monocytes and stromal cells using SPECT and CMR in a canine model of myocardial infarction. J Cardiovasc Magn Reson 2009; 11: 11.*
12. Paxinos G, Watson CR, Emson PC. *AChE-stained horizontal sections of the rat brain in stereotaxic coordinates. J Neurosci Methods 1980; 3: 129-49.*
13. Kornblum HI, Araujo DM, Annala AJ, Tatsukawa KJ, Phelps ME, Cherry SR. *In vivo imaging of neuronal activation and plasticity in the rat brain by high resolution positron emission tomography (microPET). Nat Biotechnol 2000; 18: 655-60.*
14. Handforth A, Treiman DM. *Functional mapping of the early stages of status epilepticus: a 14C-2-deoxyglucose study in the lithium-pilocarpine model in rat. Neuroscience 1995; 64: 1057-73.*
15. Fernandes MJ, Dubé C, Boyet S, Marescaux C, Nehlig A. *Correlation between hypermetabolism and neuronal damage during status epilepticus induced by lithium and pilocarpine in immature and adult rats. J Cereb Blood Flow Metab 1999; 19: 195-209.*
16. Dubé C, Boyet S, Marescaux C, Nehlig A. *Relationship between neuronal loss and interictal glucose metabolism during the chronic phase of the lithium-pilocarpine model of epilepsy in the immature and adult rat. Exp Neurol 2001; 167: 227-41.*
17. Rüschenschmidt C, Koch PG, Brüstle O, Beck H. *Functional properties of ES cell-derived neurons engrafted into the hippocampus of adult normal and chronically epileptic rats. Epilepsia 2005; 46: 174-83.*
18. Dedeurwaerdere S, Jupp B, O'Brien TJ. *Positron Emission Tomography in basic epilepsy research: a view of the epileptic brain. Epilepsia 2007; 48: 56-64.*
19. Gao F, Guo Y, Zhang H, Wang S, Wang J, Wu JM, Chen Z, Ding MP. *Anterior thalamic nucleus stimulation modulates regional cerebral metabolism: an FDG-MicroPET study in rats. Neurobiol Dis 2009; 34: 477-83.*
20. Guo Y, Gao F, Wang S, Ding Y, Zhang H, Wang J, Ding MP. *In vivo mapping of temporospatial changes in glucose utilization in rat brain during epileptogenesis: an 18F-fluorodeoxyglucose-small animal positron emission tomography study. Neuroscience 2009; 162: 972-9.*
21. Duncan JS. *Imaging and epilepsy. Brain 1997; 120 (Pt 2): 339-77.*
22. Hotta SS. *18F-labeled 2-deoxy-2-fluoro-D-glucose positron-emission tomography scans for the localization of the epileptogenic foci. Health Technol Assess (Rockv) 1998: i-vi, 1-17.*
23. Wieser HG. *PET and SPECT in epilepsy. Eur Neurol 1994; 34: 58-62.*
24. Ackermann RF, Engel J Jr, Phelps ME. *Identification of seizure-mediating brain structures with the deoxyglucose method: studies of human epilepsy with positron emission tomography, and animal seizure models with contact autoradiography. Adv Neurol 1986; 44: 921-34.*
25. Benedek K, Juhász C, Chugani DC, Muzik O, Chugani HT. *Longitudinal changes in cortical glucose hypometabolism in children with intractable epilepsy. J Child Neurol 2006; 21: 26-31.*
26. Lee JS, Asano E, Muzik O, Chugani DC, Juhász C, Pfund Z, Philip S, Behen M, Chugani HT. *Sturge-Weber syndrome: correlation between clinical course and FDG PET findings. Neurology 2001; 57: 189-95.*
27. Ourednik J, Ourednik V, Lynch WP, Schachner M, Snyder EY. *Neural stem cells display an inherent mechanism for rescuing dysfunctional neurons. Nat Biotechnol 2002; 20: 1103-10.*
28. Pluchino S, Furlan R, Martino G. *Cell-based remyelinating therapies in multiple sclerosis: evidence from experimental studies. Curr Opin Neurol 2004; 17: 247-55.*
29. Love Z, Wang F, Dennis J, Awadallah A, Salem N, Lin Y, Weisenberger A, Majewski S, Gerson S, Lee Z. *Imaging of mesenchymal stem cell transplant by bioluminescence and PET. J Nucl Med 2007; 48: 2011-20.*

http://dx.doi.org/10.3346/jkms.2015.30.9.1232